International Journal of Research Studies in Electrical and Electronics Engineering (IJRSEEE)
Volume 10, Issue 1, 2025, PP 1-8
ISSN 2454-9436 (Online)
DOI: https://doi.org/10.20431/2454-9436.1001001
www.arcjournals.org

Isotropic Radiation Pattern Antenna Using A Modified Compact Asymmetric Parallel Plate Structure

Masoud Alipour Shirazi [1], Amir Saman Nooramin [1]*, Mahdi Rahanande [2]

[1]*School of Electrical Engineering, Iran University of Science and Technology (IUST), Tehran, Iran*

[2]*School of Electrical Engineering, Babol Noshirvani University of Technology (NIT), Babol, Iran*

Corresponding Author:** ***Amir Saman Nooramin., *School of Electrical Engineering, Iran University of Science and Technology (IUST), Tehran, Iran.*

Abstract: *In this study, a quasi-isotropic antenna has been designed based on a modified asymmetric parallel plate structure. The structure is resembled to a parallel plate antenna in which a metal strip is added on the upper plate. Due to this inherent asymmetry, two orthogonal magnetic dipoles are created and a quasi-isotropic radiation pattern has been created. The radiation mechanism of this antenna is investigated in depth using the equivalent circuits and analytically. The dimension of the proposed structure is* $\mathbf{0.7\lambda \times 0.7\lambda \times 0.1\lambda}$*. A gain variation of 1.6dB with a radiation efficiency of 85% has been attained in the fractional bandwidth of 10%. Furthermore, the antenna is fabricated and the measurement results are in good agreement with the simulations.*

Key word: *quasi-isotropic radiation pattern, planar antenna, equivalent circuit, magnetic dipole.*

1. INTRODUCTION

Quasi-isotropic antennas have emerged as a promising solution in wireless communication systems, offering unique radiation patterns and coverage advantages [1]. The ability to receive electromagnetic waves in all directions can be worthy in some applications like the Internet of Things [2]. Therefore, many researches have been done to obtain spherical radiation patterns, so far [1,2].

The methods for the synthesis of quasi-isotropic radiation patterns can be categorized into two groups: conformal antennas and merging electric and magnetic dipoles. The first one has attracted less attention so far. Carl et al. used 52 Vivaldi antennas on an 18 cm diameter hemispherical structure. Consequently, an ultra-wideband dual-polarized antenna was achieved, supporting a 2-18 GHz frequency range, with a gain of approximately 18 dB, covering 120 degrees in beam-scanning [3,4]. Wang et al. proposed a bilaterally symmetric 3D quasi-isotropic antenna, wrapped in cylindrical foam. An H-shaped inductive coupling element was used to feed this antenna, obtaining a magnetic dipole and a pair of short electric dipoles. Thus, by combining orthogonal complementary dipoles with the same radiation intensity and quadrature phase differences, a quasi-isotropic radiation pattern was obtained [5]. Wang et al. used a conformal antenna array inspired by a shorted patch antenna to achieve a gain variation of 10.5 dB at 915 MHz [6]. As another example of a 3D antenna, Kirill Klionovski et al. illustrated that arranging sloped dipoles on a 3D hexagonal structure can maximize circular polarization and result in a quasi-isotropic radiation pattern. They achieved a gain of 7 dB at 1.5 GHz [7,8].

Merging electric and magnetic dipoles has attracted more attention so far. This technique utilizes two perpendicular dipole-shaped patterns, each covering the nulls of the other. The differences in the research lie in the methods used to establish electric and magnetic dipoles. Pan et al. presented a compact shorted patch antenna with a quasi-isotropic radiation pattern at 2.4 GHz [9]. As another example, Liu et al. used two broadside radiation pattern line sources to obtain a quasi-isotropic radiation pattern [10]. Lou introduced a double-sided planar angled dipole antenna that radiates broadside and utilizes two parasitic elements for end-fire radiation [11]. A dual-layered U-shaped antenna with a gain variation of 3 dB at 915 MHz was proposed by Wang et al. [12]. Kim et al. used two identical patch antennas with separate control of the phase of the two excitation ports to synthesize broadside and end-fire radiation patterns simultaneously [13]. Ali et al. presented an isotropic radiation pattern printed arc antenna at 1 GHz with a total gain variation of 3 dB [14].

Wang et al. composed a radiating patch, a fence strip resonator, and a ground plane to implement a quasi-isotropic radiation pattern antenna with a gain variation of more than 6dB [15]. [16] proposed an antenna consisting of four monopoles and a sequential 90-degree phase shift feed network for each monopole arm. A gain variation of 6 dB at 1 GHz was obtained. Two perpendicularly positioned split ring resonators were used in [17] to obtain a quasi-isotropic circularly polarized radiation pattern with a gain variation of 3 dB. [18], with the goal of achieving an isotropic radiation pattern, used two perpendicularly positioned electrically small spherical antennas. [19] presents a wide-band isotropic radiation pattern antenna with the gain of 4.8 dB at 900 MHz. Using an inclined central part modified dipole, Niamen et al. [20] presented a single-feed planar multi-band quasi isotropic antenna. The antenna covers the frequency band of 815-1095 MHz and 1650-2090 MHz with a gain variation of 7.7dB and 10dB at the 940 and 1800 MHz, respectively.

In fact, an exact isotropic radiation pattern may be useless in some cases due to feeding considerations, as backside radiation is not desired in certain scenarios. This paper describes the design of an asymmetric parallel plate antenna with a quasi-isotropic radiation pattern capable of adjusting the beam width and radiation pattern. In Section II, the antenna design structure is explained. Then, in Section III, the theory of the radiation mechanism is discussed. Section IV is devoted to the simulation and measurement results. Finally, some conclusions are presented.

2. ANTENNA DESIGN

Fig. 1 illustrates the configuration of the proposed quasi-isotropic antenna. The 3D view, front and back view, and side view are depicted in Fig. 1(a) to Fig. 1(c), respectively. The antenna is divided into three main parts, each illustrated with numbers 1, 2, and 3 in Fig. 1. It can be seen that the antenna comprises two parallel plates. The upper plate (1) consists of a 20 mil Rogers RO4003C substrate, with circular and rectangular patches printed on the back and front sides, respectively. A brass hollow core cylinder is attached to the circular patch (2). As shown later, this section is used for impedance matching. A circular metallic plate is used for the lower plate (3).

All other parameters and values in Fig. 1 are presented in Table 1.

Table.1 *Antenna Parameters*

Parameter	Value	Parameter	Value
h	**0.7[cm]**	**gap**	**0.8[cm]**
d	**1.3[cm]**	**width**	**6[cm]**
Ri	**0.1[cm]**	**length**	**5[cm]**
Ro	**1[cm]**	**X**	**7[cm]**
R	**3[cm]**	**Y**	**3[cm]**
L	**10[cm]**	ε_r	**3.55**

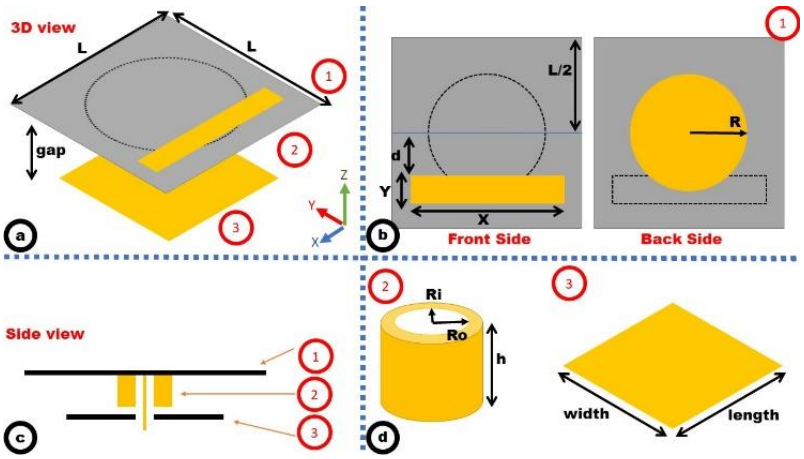

Figure1. Antenna Structure. (a)3D view of antenna. (b)Front side and back side of the PCB mentioned as number (1) in Fig. 1 a) and Fig. 1 (c). (c)Side view of antenna. (d)Parameters of brass ring and conducting plate are shown with numbers (2) and (3) respective

3. THE MECHANISM OF RADIATION

As can be seen in the antenna 3D view in Fig. 1, the structure is symmetric in the XZ plane and non-symmetric in the YZ plane. The equivalent circuit of the antenna on XZ and YZ planes is depicted in Fig. 2. Where, R_r is radiation resistance, Z_s is impedance of source, Z_{c2} is the parallel plate waveguide impedance, and Z_{c1} which is placed between feed and parallel plate waveguide, is responsible for impedance matching between feed and waveguide. The brass ring is modeled as the Z_{c1}. The radius of the plates, are about half of the wavelength at 3 GHz. Therefore, as depicted in Fig. 3, on the symmetric plane (XZ plane), two edges of the upper plate would have the same amplitude and opposite phases. Therefore, two magnetic currents M_{sl} and M_{sr} can be considered.

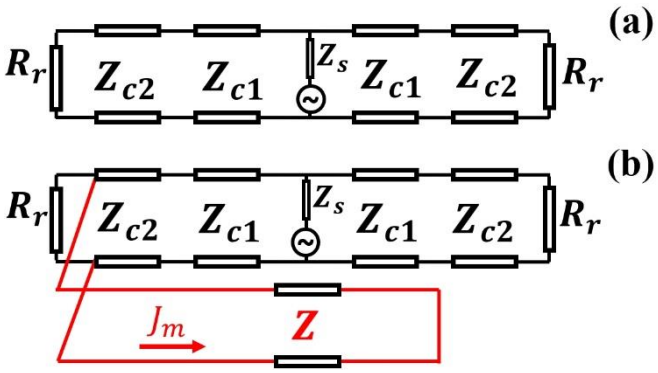

Figure 2 *Antenna Equivalent Circuit on (a)YZ-plane, (b)XZ-plane*

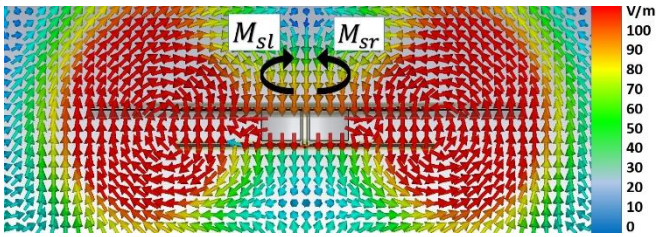

Fig3 *E-field on XZ plane*

Alternating E-field on the left edge and right edge can be modeled as magnetic currents as follows,

$$\begin{cases} \vec{M} = -\hat{n} \times \vec{E} \\ \vec{E} = E_0 \cos(\omega t)\, \hat{a}_z \end{cases} \quad (1)$$

We have:

$$\vec{E} = E_0 \cos(\omega t)\, \hat{a}_z, \hat{n} = -\hat{y} \quad (2)$$

Therefore, the magnetic current for the right edge can be expressed as:

$$\vec{J}_{mr} = -E_0 \cos(\omega t)\, \hat{a}_x \quad (3)$$

Similarly, for the left edge:

$$\vec{J}_{ml} = E_0 \cos(\omega t)\, \hat{a}_x \quad (4)$$

Due to the symmetry of the antenna structure in the XZ plane, equations (3) and (4) can be written in spherical coordinates as follows,

$$\vec{M} = E_0 \cos(\omega t)\, \hat{a}_{\emptyset} \tag{5}$$

Therefore, the vector potential $\vec{F}$ would be:

$$\vec{F} = \frac{\varepsilon}{4\pi} \int M_{\emptyset} \frac{e^{-j\beta R}}{R} dl' \tag{6}$$

Where, dl' can be obtained as:

$$dl' = r d\emptyset' = \frac{\lambda}{4} d\emptyset' \tag{7}$$

So $\vec{F}$ can be written as:

$$\vec{F} = \frac{\varepsilon\lambda}{8} E_0 \cos(\omega t) \frac{e^{-j\beta R}}{R} \hat{a}_{\emptyset} \tag{8}$$

Having $\vec{F}$, $\vec{H}$ can be obtained as follows,

$$\vec{H} = -j\omega \frac{\varepsilon\lambda}{8} E_0 \cos(\omega t) \frac{e^{-j\beta R}}{R} \hat{a}_{\emptyset} \tag{9}$$

We have:

$$\vec{E} = -\frac{1}{\varepsilon} \nabla \times \vec{F} \tag{10}$$

So, electric field can be obtained from eq.11 and eq.12:

$$E_r = \frac{\lambda}{8} E_0 \cos(\omega t) \frac{\cos(\theta)}{\sin(\theta)} \frac{e^{-j\beta R}}{R^2} \tag{11}$$

And

$$E_{\theta} = -j\beta \frac{\lambda}{8} E_0 \cos(\omega t) \frac{e^{-j\beta R}}{R} \tag{12}$$

Due to spherical attenuation of $\frac{1}{R^2}$, component E_r is negligible in far fields:

$$H_{\emptyset sym} = -j\omega \frac{\varepsilon\lambda}{8} E_0 \cos(\omega t) \left[\frac{1}{r} + a\left(\frac{j\beta}{r} + \frac{1}{r^2}\right) \sin(\theta) \cos(\omega t)\right] \tag{13}$$

$$E_{\emptyset sym} = -j\beta \frac{\lambda}{8} E_0 \cos(\omega t) \left[\frac{1}{r} + a\left(\frac{j\beta}{r} + \frac{1}{r^2}\right) \sin(\theta) \cos(\omega t)\right] \tag{14}$$

As a simpler and shorter solution using eq.3 and eq.4, an array of two magnetic currents are placed beside each other with the distance of $(d = \frac{\lambda}{2})$ having phase shift of 180°, therefore the radiation pattern can be obtained as follows,

$$AF = \cos\left[\frac{1}{2}(kd\cos(\theta) + \pi)\right] \quad (15)$$

The magnetic current in the XY plane, generates a z-direction dipole shaped radiation pattern. So, to achieve a quasi-isotropic radiation pattern, an orthogonal magnetic current is needed. By using a patch on the right side of the upper plate, the symmetry of the antenna is disrupted in the YZ plane, leading to the creation of an additional magnetic current in that plane. It is known that the electric field is always perpendicular to any conducting surface. Therefore, by adding a conducting patch on the right side of the upper plate, the electric field vector rotates to satisfy the boundary condition. So, the electric field on one edge would be tangential and on the other edge would be perpendicular to the plate. Therefore, a magnetic current will be produced (red dashed line in Fig. 4).

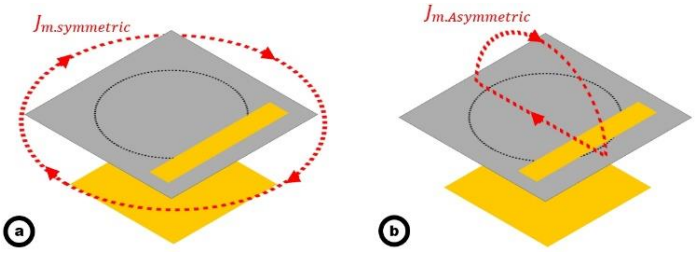

Fig4. *The Equivalent Magnetic Currents Distributions (a) Due to symmetricity (b) Due to assyemetricity*

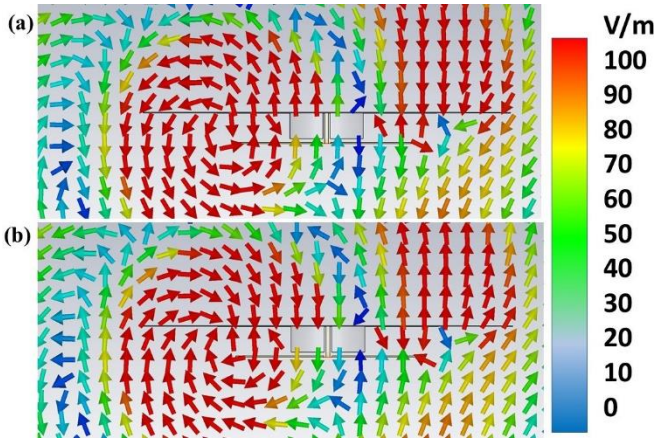

Figure5. *E-field on YZ plane. ωt= (a)=0°,(b)=180°*

As can be seen in Fig.5 (a) and Fig. 5(b), the electric field rotates in the YZ plane, and it can be modeled as a magnetic current in that plane. The difference for the non-symmetric plane (YZ-plane) is 90° rotation compared to the symmetric plane (XZ-plane). So, from Eq.13 and Eq.14, $\vec{E}$ and $\vec{H}$ for non-symmetric plane, can be written as:

$$H_{\emptyset non.sym} = -j\omega\frac{\varepsilon\lambda}{8}E_0\cos(\omega t)\left[\frac{1}{r} + a(\frac{j\beta}{r} + \frac{1}{r^2})\cos(\theta)\cos(\omega t)\right] \quad (16)$$

$$E_{\emptyset non.sym} = -j\beta\frac{\lambda}{8}E_0\cos(\omega t)\left[\frac{1}{r} + a(\frac{j\beta}{r} + \frac{1}{r^2})\cos(\theta)\cos(\omega t)\right] \quad (17)$$

4. Simulation And Measurement Results

The estimated total electric field according to Eq.18 on the assumption of Eq.14 and Eq.17 can be calculated as,

$$\vec{E}_{Total} \cong \vec{E}_{non.sym} + \vec{E}_{sym} \qquad (18)$$

As depicted in Fig. 6, the antenna is fabricated and experimentally tested in an anechoic chamber. Simulation and measurement result of the return loss are shown in Fig. 7. The estimated total electric field based on Eq.18, simulation, and the measured results in the XZ and the XY-planes are depicted in Fig. 8 (a) and Fig.8 (b), respectively.

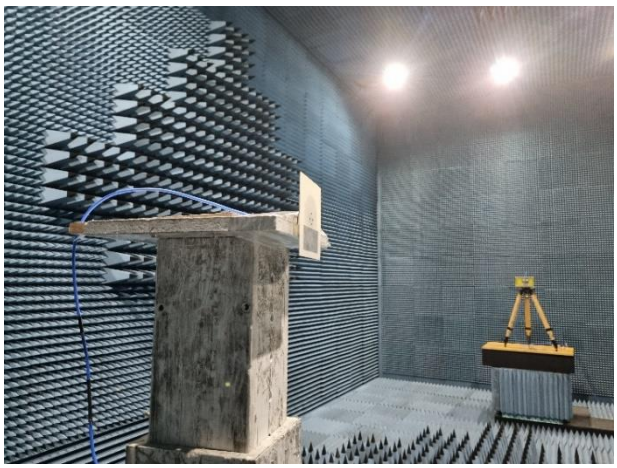

Figure6. *The Measurement Setup*

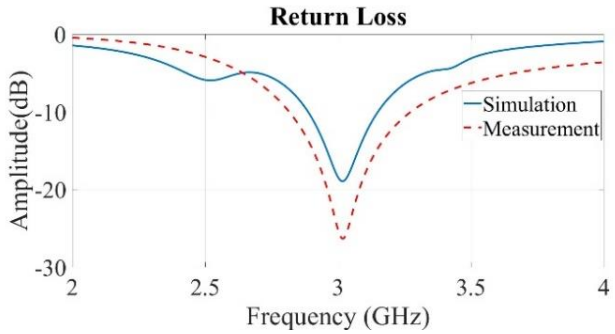

Figure7. *Return Loss*

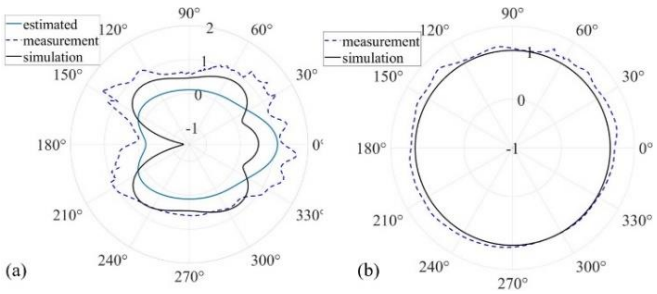

Figure8. *Electric Field Pattern (a) XZ-plane (b) XY-plane*

Fig. 9 (a) depicts the 3D radiation pattern of the antenna, showing the nearly spherical radiation pattern. The gain variation in the XY-plane is shown in Fig. 9 (b). It worth mentioning that due to antenna holder consideration, the measurement gain results in the range of $[150 - 180]°$ is inaccurate. The maximum gain is 1.28 dB, and the minimum gain is -0.37 dB, resulting in a gain variation of 1.65 dB. The comparison of the maximum gain and the maximum directivity of the antenna in the simulation process, shows that the efficiency is about 85%.

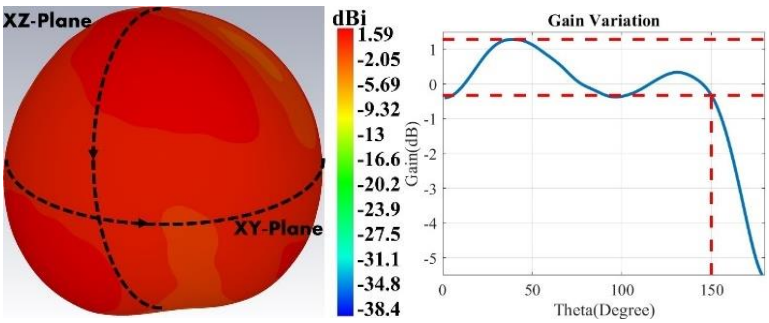

Figure9. *(a) Antenna 3D Pattern (b) Gain Variation*

One of the outstanding features of the proposed antenna is its capability to adjust the beam-width and radiation pattern by changing the size of lower conducting plate which was shown in Fig. 1 (d). In Fig. 10, the black line and the blue line are used for the gain on the assumption of a $(5cm \times 6cm)$ and $(10cm \times 12cm)$ lower conducting plate, respectively.

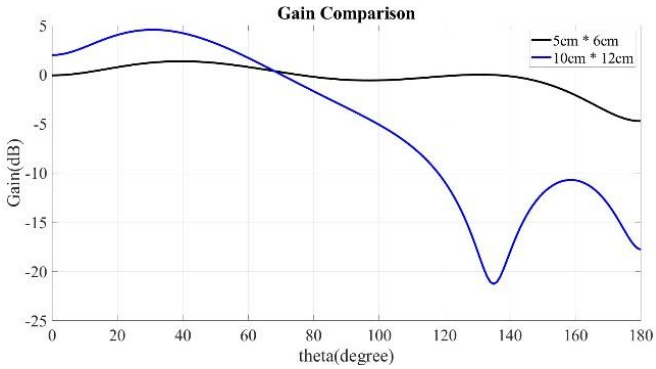

Figure10. *Gain Comparison*

As shown in Fig. 10, the higher gain and lower beam width belongs to wider conducting plate.

Table. 2, shows a brief comparison of the gain variation for the proposed antenna and related recent research. In this table, GV, F, and n.m stand for gain variation, frequency and not mentioned respectively.

Table 2. *The Comparison of Proposed Antenna Parameters and Those Reported in Literature*

Ref	GV (dB)	Efficiency	Dimension (λ^3)	F (GHz)
(5)	3.53	n.m	$0.05 \times 0.05 \times 0.125$	2.5
(6)	10.5	n.m	$0.3 \times 0.15 \times 0.0025$	0.915
(7)	7	n.m	$0.18 \times 0.18 \times 0.13$	0.925
(9)	1.88	90%	$0.22 \times 0.22 \times 0.006$	2.45
(10)	3.6	n.m	$0.2 \times 0.2 \times 0.003$	1
(11)	2.59	90%	$0.29 \times 0.28 \times 0.016$	2.4
(12)	3	n.m	$0.12 \times 0.13 \times 0.003$	0.915
(13)	6.8	n.m	$0.8 \times 0.8 \times 0.08$	2.4
(14)	0.5	86%	$0.203 \times 0.25 \times 0.003$	1
(15)	6.88	84%	$0.28 \times 0.28 \times 0.042$	2.45
(16)	6	n.m	$0.23 \times 0.23 \times 0.0017$	1
(17)	3	n.m	$0.19 \times 0.15 \times 0.15$	0.750
(19)	6.8	87%	$0.18 \times 0.18 \times 0.13$	0.925
(20)	7.7	95%	$0.5 \times 0.5 \times 0.003$	0.915
This Work	1.65	85%	$0.7 \times 0.7 \times 1$	3

5. CONCLUSION

In this paper, we proposed a quasi-isotropic antenna and explained the mechanism of radiation. The antenna is comprised of a parallel plate structure, which is loaded by a metal strip on the upper plate and shown that two orthogonal magnetic currents are created due to the asymmetric nature of the structure. Furthermore, an equivalent circuit is introduced to explain the radiation mechanism. Based

on the simulation and measurement results, a gain variation of 1.6 dB and a relative bandwidth of 10% are achieved. The short electrical dimensions of the antenna in addition to the planar structure make it a suitable option in array applications.

REFERENCES

[1] Shah, Syed Imran Hussain, et al. "Recent advancements in quasi-isotropic antennas: A review." IEEE Access 9 (2021): 146296-146317.

[2] Ta, Son Xuat, Ikmo Park, and Richard W. Ziolkowski. "Crossed dipole antennas: A review." IEEE Antennas and Propagation Magazine 57.5 (2015): 107-122.

[3] Pfeiffer, Carl, and Jeffrey Massman. "An UWB hemispherical Vivaldi array." IEEE Transactions on Antennas and Propagation 70.10 (2022): 9214-9224.

[4] Pfeiffer, Carl, and Jeffrey Massman. "A UWB Low-Profile Hemispherical Array for Wide Angle Scanning." IEEE Transactions on Antennas and Propagation (2022).

[5] Wang, Yanyang, and Sen Yan. "Design of an electrically small 3-D antenna with quasi-isotropic radiation pattern." IEEE Antennas and Wireless Propagation Letters 20.10 (2021): 1873-1877.

[6] Wang, Yanyang, Sen Yan, and Binke Huang. "Conformal folded inverted-F antenna with quasi-isotropic radiation pattern for robust communication in capsule endoscopy applications." IEEE Transactions on Antennas and Propagation 70.8 (2022): 6537-6550

[7] Su, Zhen, et al. "A Fully-Printed 3D Antenna With 92percent Quasi-Isotropic and 85 percent CP Coverage." IEEE Transactions on Antennas and Propagation 70.9 (2022): 7914-7922.

[8] Klionovski, Kirill, Enrica Martini, and Stefano Maci. "An Antenna with a Modulated Self-Complementary Metasurface Ground Plane for GPS Applications." 2023 17th European Conference on Antennas and Propagation (EuCAP). IEEE, 2023.

[9] Pan, Yongmei, and Shaoyong Zheng. "A compact quasi-isotropic shorted patch antenna." IEEE Access 5 (2017): 2771-2778.

[10] Liu, Peiqin, and Yue Li. "Quasi-isotropic radiation pattern synthesis using triple current line sources." IEEE Transactions on Antennas and Propagation 68.12 (2020): 8150-8155.

[11] Luo, Jia Wen, et al. "A planar angled-dipole antenna with quasi-isotropic radiation pattern." IEEE Transactions on Antennas and Propagation 68.7 (2020): 5646-5651.

[12] Wang, Ren, et al. "Low-profile implementation of U-shaped power quasi-isotropic antennas for intra-vehicle wireless communications." IEEE Access 8 (2020): 48557-48565.

[13] Kim, Jonghyun, et al. "A symmetrically stacked planar antenna concept exhibiting quasi-isotropic radiation coverage." IEEE Antennas and Wireless Propagation Letters 19.8 (2020): 1390-1394.

[14] Ali, Hafiz T., et al. "Design and development of a near isotropic printed arc antenna for direction of arrival (DoA) applications." Electronics 10.7 (2021): 797.

[15] Wang, Yanyang, and Sen Yan. "A compact in-band full duplexing antenna with quasi-isotropic radiation pattern for IoT-based smart home and intravehicle wireless communication applications." IEEE Internet of Things Journal 9.17 (2022): 16689-16700.

[16] Zhang, Yongjian, and Yue Li. "Wideband Isotropic Antenna With Miniaturized Ground for Enhanced 3 dB Coverage Ratio." IEEE Antennas and Wireless Propagation Letters 21.6 (2022): 1253-1257

[17] Wang, Yang, et al. "An Electrically Small Antenna with Quasi-Isotropic Coverage for Linearly Polarized Receiver." IEEE Transactions on Antennas and Propagation 70.12 (2022): 11559-11568.

[18] Liao, Hanguang, and Atif Shamim. "A Novel Dual-band Electrically Small Quasi-isotropic Antenna." 2023 17th European Conference on Antennas and Propagation (EuCAP). IEEE, 2023.

[19] Wang, Ruiqi, Kirill Klionovski, and Atif Shamim. "Fully Printed 3D Antennas with Wideband Radiation Isotropy Based on Annular Currents Models." IEEE Open Journal of Antennas and Propagation (2023).

[20] Niamien, Constant MA. "Single-feed planar multiband quasi-isotropic antennas through collocating and co-design approaches." IEEE Transactions on Antennas and Propagation 71.4 (2023): 2974-2988.

Citation: *Amir Saman Nooramin et.al., (2025) "Isotropic Radiation Pattern Antenna Using A Modified Compact Asymmetric Parallel Plate Structure", International Journal of Research Studies in Electrical and Electronics Engineering (IJRSEEE), 10(1), pp.1-8, DOI: https://doi.org/10.20431/2454-9436.1001001.*